Spatial and spectral shape of inhomogeneous nonequilibrium exciton-polariton condensates

Michiel Wouters,[1] Iacopo Carusotto,[2] and Cristiano Ciuti[3]
[1]*TFVS, Universiteit Antwerpen, Groenenborgerlaan 171, 2020 Antwerpen, Belgium*
[2]*BEC-CNR-INFM and Dipartimento di Fisica, Università di Trento, I-38050 Povo, Italy*
[3]*Laboratoire Matériaux et Phénomènes Quantiques, Université Paris Diderot-Paris 7 and CNRS, UMR 7162, Bâtiment Condorcet, 75205 Paris Cedex 13, France*
(Received 8 September 2007; published 20 March 2008)

We develop a mean-field theory of the spatial profile and the spectral properties of polariton condensates in nonresonantly pumped semiconductor microcavities in the strong coupling regime. Specific signatures of the nonequilibrium character of the condensation process are pointed out: a striking sensitivity of the condensate shape on the optical pump spot size is demonstrated by analytical and numerical calculations, in good quantitative agreement with recent experimental observations.

DOI: 10.1103/PhysRevB.77.115340 PACS number(s): 05.30.Jp, 03.75.Kk, 42.65.Sf, 71.36.+c

I. INTRODUCTION

Convincing evidences of Bose-Einstein condensation (BEC) in a solid-state system have been recently reported in a gas of exciton-polaritons in a semiconductor microcavity in the strong coupling regime.[1–8] In addition to being a remarkable example of an exciton condensate, this system opens interesting perspectives toward the study of the BEC phenomenon in completely different regimes. Polariton condensates differ in several fundamental aspects from the ideal case generally considered in textbooks: polariton-polariton interactions are significant and the system is far from thermodynamical equilibrium.[9] While the separate effect on condensation of the interactions and of the nonequilibrium condition is already well understood from either ultracold atom[10] or laser[11] theory, not much is yet known about the interplay of the two effects when simultaneously present. In this case, the Bose gas is, in fact, a quantum degenerate, interacting many-body system whose stationary state does not correspond to a thermal equilibrium state, but rather originates from a dynamical balance of pumping and losses.[12–14]

Some striking consequences of the nonequilibrium condition on the elementary excitations have been recently predicted, with the propagating sound mode of equilibrium condensate being, e.g., replaced by a diffusive mode.[13,14] Even more remarkable, an unexpectedly rich behavior has been observed in recent experiments in the spatial and spectral shapes of the condensate depending on the size of the pump spot.[1,2] While at equilibrium BEC generally occurs at zero momentum and the trapping potential is only responsible for the k-space broadening due to finite size,[10] the first experimental studies of polariton condensates performed with a relatively small pump laser spot showed Bose-Einstein condensation into a ring of momentum states with a nonzero wave vector;[1] mutual coherence of different k states was, however, interferrometrically demonstrated, which proved that a true condensate was created, and not a fragmented one.[15] Standard condensation around $k=0$ was then recovered in later experiments using a much wider excitation spot.[2,3] So far, most of these experimental observations have challenged theoretical understanding:[16] the purpose of the present paper is to propose a complete and unified theoretical model able to explain them in a simple and physically transparent way.

Our work is based on a mean-field study of nonequilibrium condensates, which takes explicitly into account the effect of the spatially finite pump spot by means of a generalized Gross–Pitaevskii equation (GPE) as developed in Ref. 14. As compared to kinetic approaches based on the Boltzmann equation,[17–21] our model fully includes the coherence of the polariton field; as compared to single-mode theories,[22,23] it is able to follow the spatial, i.e., multimode, dynamics of the condensate. Both these features are, indeed, essential to get a reliable theoretical description of the nonequilibrium Bose-Einstein condensation process for generic pump laser geometries and in the presence of a microcavity disorder potential. As long as the mean-field approximation is accurate, solving the GPE provides complete information on the shape of the polariton condensate in both real and momentum space, as well as on its spectral properties under a pulsed excitation. The formal similarities with the equations appearing in the context of pattern formation in nonlinear dynamical systems far from equilibrium,[24] in particular, hydrodynamical[25] and nonlinear optical[26] ones, are of great utility to obtain a physical understanding of the complicated spatial structures that appear as a consequence of the interplay of inhomogeneity, nonlinearity, driving, and dissipation.

The paper is organized as follows. In Sec. II, we give a short review of the generalized nonequilibrium Gross–Pitaevskii model recently developed in Ref. 14. This theory is applied in the following sections to obtain predictions for the stationary state of the nonequilibrium condensate under the combined effect of pumping and losses, and to explain the experimental observations in different excitation geometries. The main features of the large pump spot case are described in Sec. III: as a consequence of repulsive interactions, polaritons condense in a state with an outward flow pattern and a nontrivial radial phase profile. The effect of disorder on such a nonequilibrium condensate is investigated in Sec. IV: the flow pattern is partially perturbed by the disorder potential, but the nontrivial phase profile is still apparent as the **k**-space pattern is no longer centrosymmetric and the main peak is found at finite **k**. Condensation in the small excitation spot case is discussed in Sec. V: as observed in the experiments, the condensate now sits on a ring in **k** space

corresponding to polaritons being ballistically ejected out of the excitation spot by the repulsive interactions. The robustness of all these effects with respect to the presence of noncondensed polaritons has been verified in Sec. VI by means of Wigner–Monte Carlo calculations. Conclusions and perspectives are finally summarized in Sec. VII.

II. MEAN-FIELD MODEL

As we have shown in detail in a recent paper,[14] a good mean-field description of the dynamics of the condensate macroscopic wave function $\psi(\mathbf{r})$ is obtained from a generalized Gross–Pitaevskii equation of the following form:

$$i\hbar\frac{\partial\psi(\mathbf{r})}{\partial t}=\left\{E_0-\frac{\hbar^2}{2m}\nabla_{\mathbf{r}}^2+\frac{i\hbar}{2}[R[n_R(\mathbf{r})]-\gamma_c]+V_{ext}(\mathbf{r})+\hbar g|\psi(\mathbf{r})|^2+V_R(\mathbf{r})\right\}\psi(\mathbf{r}), \tag{1}$$

where $E_0=\hbar\omega_0$ and m, respectively, are the minimum and the effective mass of the lower polariton branch, and $g>0$ quantifies the strength of repulsive binary interactions between condensate polaritons.[12,27] Whenever needed, exciton and cavity disorder can be included as an external potential term $V_{\text{ext}}(\mathbf{r})$.[28] Condensate polaritons have a linear loss rate γ_c and are continuously replenished by stimulated emission from the polariton reservoir created by the nonresonant optical pump. At the simplest level, the corresponding gain rate $R[n_R]$ can be described by a monotonically growing function of the local density $n_R(\mathbf{r})$ of reservoir polaritons in the so-called bottleneck region.[17] At the same time, the reservoir produces a mean-field repulsive potential $V_R(\mathbf{r})$ that can be approximated by the linear expression $V_R(\mathbf{r})\simeq\hbar g_R n_R(\mathbf{r})+\hbar\mathcal{G}P(\mathbf{r})$, where $P(\mathbf{r})$ is the (spatially dependent) pumping rate and $g_R,\mathcal{G}>0$ are phenomenological coefficients to be extracted from the experiment.[29] The GPE equation (1) for the condensate then has to be coupled to a rate equation for $n_R(\mathbf{r})$ as follows:

$$\dot{n}_R(\mathbf{r})=P(\mathbf{r})-\gamma_R n_R(\mathbf{r})-R[n_R(\mathbf{r})]|\psi(\mathbf{r})|^2. \tag{2}$$

Polaritons are injected into the reservoir at a rate $P(\mathbf{r})$ and relax at an effective rate[30] $\gamma_R\gg\gamma_c$. Depletion of the reservoir density due to the stimulated emission into the condensate mode is taken into account by the $R[n_R(\mathbf{r})]|\psi(\mathbf{r})|^2$ term.

III. LARGE EXCITATION SPOT

A. Spatially homogeneous system

In the homogeneous case, i.e., under a spatially uniform pumping and in the absence of any external potential, Eqs. (1) and (2) admit simple analytical stationary solutions.[14] Below the threshold, the condensate density remains zero $|\psi|^2=0$, while the reservoir one grows linearly with the pump intensity, $n_R=P/\gamma_R$. At the threshold pump intensity P^{th}, the stimulated emission rate exactly compensates the losses $R[n_R^{th}]=\gamma_c$ and the empty condensate solution with $\psi=0$ becomes dynamically unstable. Above the threshold, the reservoir density is homogeneous $n_R(\mathbf{r})=n_R$ and the condensate wave function is of the form $\psi(\mathbf{r})=e^{i(\mathbf{k}_c\cdot\mathbf{r}-\omega_c t)}\psi_0$. Inserting this ansatz into the motion equation, we find that n_R is clamped at the threshold value n_R^{th}, while the condensate density grows as $|\psi_0|^2=(P-P^{th})/\gamma_c$. The condensate wave vector $\mathbf{k}_c$ remains so far undetermined, and stable solutions with arbitrary values of $\mathbf{k}_c$ exist. As we shall see in what follows, the specific solution that is actually chosen by a given physical system depends on the boundary conditions to be imposed at the edges of the pump spot. For each value of $\mathbf{k}_c$, the oscillation frequency ω_c is finally fixed by the following state equation:

$$\omega_c-\omega_0=\frac{\hbar k_c^2}{2m}+g|\psi_0|^2+g_R n_R+\mathcal{G}P. \tag{3}$$

B. Local density approximation

The physics is much richer in the presence of an inhomogeneous intensity profile $P(\mathbf{r})$ of the pump. In this case, we can still look for stationary solutions of the following form:

$$\psi(\mathbf{r},t)=\psi_0(\mathbf{r})e^{-i\omega_c t}=\sqrt{\rho(\mathbf{r})}e^{i[\phi(\mathbf{r})-\omega_c t]}, \tag{4}$$

$$n_R(\mathbf{r},t)=n_R(\mathbf{r}), \tag{5}$$

where $\rho(\mathbf{r})$ and $\phi(\mathbf{r})$ are the local density and phase of the condensate wave function $\psi(\mathbf{r})=\sqrt{\rho(\mathbf{r})}\exp[i\phi(\mathbf{r})]$. The condensate frequency ω_c is the same at all points, while the local condensate wave vector $\mathbf{k}_c(\mathbf{r})$ is defined as the spatial gradient of the condensate phase $\mathbf{k}_c(\mathbf{r})=\nabla_{\mathbf{r}}\phi(\mathbf{r})$. Inserting the forms (4) and (5) into the equations of motion (1) and (2) and imposing stationarity of the solution, one obtains the following set of conditions:

$$\hbar\omega_c=\hbar\omega_0+\frac{\hbar^2k_c^2}{2m}+V_{ext}+\frac{\hbar^2}{2m}\frac{\nabla_{\mathbf{r}}^2\sqrt{\rho}}{\sqrt{\rho}}+\hbar g\rho+\hbar g_R n_R+\hbar\mathcal{G}P, \tag{6}$$

$$0=[R[n_R]-\gamma_c]\rho-\frac{\hbar}{m}\nabla_{\mathbf{r}}\cdot\rho\mathbf{k}_c, \tag{7}$$

$$P=\gamma_R n_R+R[n_R]\rho. \tag{8}$$

Provided the spatial variation of the pump profile $P(\mathbf{r})$ is smooth enough, one can perform a kind of local density approximation (LDA), where the quantum pressure term (proportional to $\nabla_{\mathbf{r}}^2\sqrt{\rho}$) in Eq. (6) and the current divergence term in Eq. (7) are neglected. Within this LDA approach, the condensate density profile $\rho(\mathbf{r})$ is equal to the one of an homogeneous system with the local value of the pump intensity $P(\mathbf{r})$. In particular it vanishes for $\rho(\mathbf{r})=0$ at all points $\mathbf{r}$ where $P(\mathbf{r})$ is below the threshold $P(\mathbf{r})<P_{th}$. The determination of the condensate wave vector $\mathbf{k}_c$ and, consequently, of the condensate frequency ω_c are more complicated: as the oscillation frequency ω_c of the condensate is constant in space, the variation of $P(\mathbf{r})$ across the pump spot must be, in fact, compensated by a corresponding spatial variation of the local wave vector $\mathbf{k}_c(\mathbf{r})$.

An analytic solution can be explicitly worked out for the simplest case of a circularly symmetric pump profile $P(r)$ in

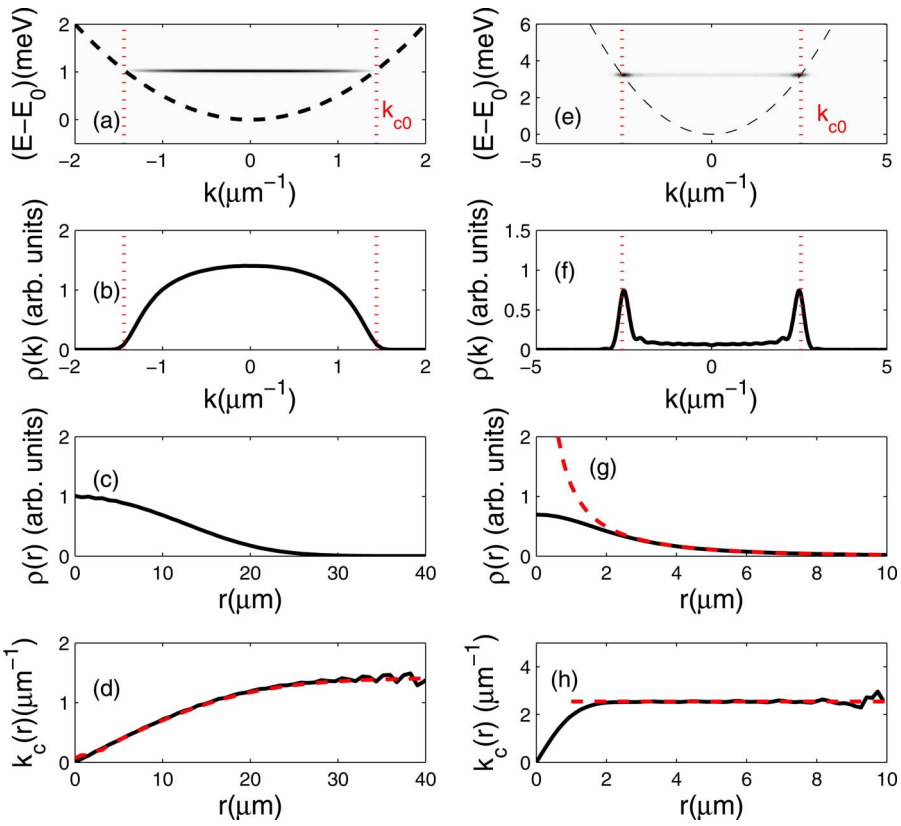

FIG. 1. (Color online) Numerical results of generalized GPE simulations in the absence of disorder for [(a)–(d)] a large $\sigma_p=20$ μm and [(e)–(h)] a small $\sigma_p=2$ μm circular excitation pump spot, respectively. (a) and (e) give the (k,E) emission pattern, (b) and (f) the polariton distribution in momentum space, (c) and (g) the polariton distribution in real space, and (d) and (h) the local wave vector $k_c(r)$. The wave vector k_{c0} of a free polariton at ω_c is indicated by the dotted lines in (a), (b), (e), and (f); the dashed line in (g) is the analytical approximations to the density tail, and the dashed lines in (d) and (h) are the LDA predictions to the local wave vector. All quantities in real (momentum) space depend only on the radial coordinate $r=|\mathbf{r}|$ $(k=|\mathbf{k}|)$. The values of the parameters used in the simulations are as follows: $\hbar g=0.015$ meV μm^2, $\hbar\gamma_c=0.5$ meV, $\hbar\gamma_R=2$ meV, $\hbar R[n_R]=(0.05$ meV μm$^2)\times n_R\hbar g_R=0$, $\mathcal{G}=0.0175$ μm^2, and $P/P_{th}=2$ (left panels) and $P/P_{th}=8$ (right panels).

the absence of disorder $V_{ext}=0$. In this case, we can look for cylindrically symmetric stationary solutions where the condensate frequency ω_c is determined by the condition that the local condensate wave vector vanishes $\mathbf{k}_c(r=0)=0$ at the center of the spot, i.e.,

$$\omega_c-\omega_0=g\rho(r=0)+g_Rn_R(r=0)+\mathcal{G}P(r=0). \tag{9}$$

For standard (e.g., Gaussian or top-hat) pump spots with a monotonically decreasing intensity profile along the radial direction, the local wave vector $\mathbf{k}_c$ is in the radial direction and its modulus k_c monotonically grows with r, reaching its maximal value at the condensate edge where $P(r)=P_{th}$. The repulsive interactions create, in fact, an antitrapping potential as follows:

$$V_{at}(r)=\hbar g\rho(r)+\hbar g_Rn_R(r)+\hbar\mathcal{G}P(r), \tag{10}$$

which ballistically accelerates the condensate polaritons away from the center: the state equation (3) describes the conservation of the mechanical energy during the flow. The boundary condition that no polariton flux can enter the condensate from the external region where no pumping is present fixes the direction of $\mathbf{k}_c$ to be along the outward radial direction.

In order to verify the robustness of these analytical considerations and, in particular, assess the dynamical stability of this solution for the typical values of the experimental parameters, extensive numerical simulations of the GPE equation (1) coupled to the reservoir evolution equations (2) have been performed for a wide range of pump parameters.

C. Numerical results for a large excitation spot

The case of a cw pump with a wide Gaussian spot of waist $\sigma_p=20$ μm is described in the four plots in the left column of Fig. 1. The parameters of the pump are chosen in a way to reproduce the experimentally observed[2] value of the blueshift of the emission frequency $\omega_c-\omega_0$ of the order of 1 meV. As expected, the long-time dynamics of the system tends to a dynamically stable steady state with a single oscillation frequency ω_c and a stationary reservoir density profile.[31] Differently from the spatially homogeneous case where condensation can take place in many modes with different $\mathbf{k}$ vectors depending on the initial conditions of the

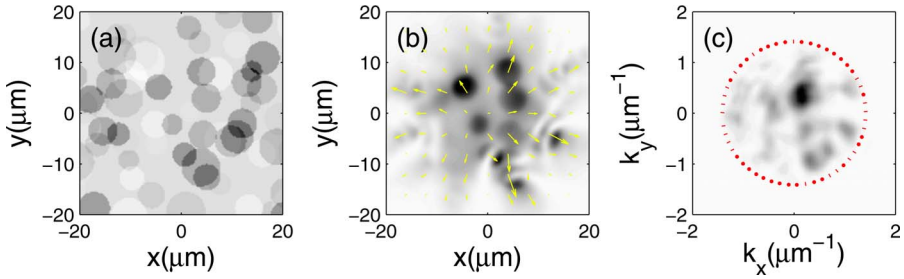

FIG. 2. (Color online) Numerical GPE simulations for a large pump spot in the presence of disorder. (a) Disorder potential (gray scale with 1 meV range), polariton distribution in two-dimensional (b) real and (c) momentum space. The arrows in (b) indicate the polariton current. The radius of the dotted circle in (c) is the free polariton wave vector k_{c0}. Same parameters as in Figs. 1(a)–1(d).

GPE evolution, the condensate mode is here completely determined by the geometry of the finite size pumping spot.

In agreement with the previous analytical discussion, the k-space distribution [Fig. 1(b)] is contained in the $k<k_{c0}$ region ($\hbar k_{c0}^2/2m=\omega_c-\omega_0$), delimited by the free particle dispersion [vertical dashed lines in Fig. 1(b)]. Still, the broadening of the condensate momentum distribution due to the ballistic acceleration largely exceeds the finite size broadening predicted by the Heisenberg position-momentum uncertainty principle and reflects the complex phase profile of the condensate mode. This is in stark contrast with the case of equilibrium condensates,[10] where symmetry under time reversal makes the condensate phase in the ground state uniform throughout the whole cloud and the local wave vector to be $\mathbf{k}_c=0$ everywhere.

To further confirm our interpretation of the $\mathbf{k}$-space broadening observed in the simulations, we have compared the numerical result for the local wave vector $\mathbf{k}_c$ with the LDA prediction discussed in the previous section. The two are plotted in Fig. 1(d) as a full and a dashed line, respectively: the agreement between the two is excellent everywhere.

IV. EFFECT OF DISORDER

Although this simple calculation is able to correctly account for the main observations, some experimental features are still missing: as one can see in Fig. 8.9 of Ref. 32, some structures are, in fact, present on top of the broad profile shown in Figs. 1(a) and 1(b), in particular, a narrow peak centered at a finite $\mathbf{k}\neq 0$ momentum.

To explain these features, we have performed GPE simulations including a weak disorder potential $V_{ext}(\mathbf{r})$ acting on polaritons. Figure 2 gives an example of the outcome for a given realization of the disorder potential, constructed as an ensemble of circular defects [Fig. 2(a)].

The $\mathbf{k}$-space emission shown in Fig. 2(c) is still mostly contained in the $k<k_{c0}$ circle as in the clean system case, but a significant specklelike modulation appears on top of the regular background, with a few dominating narrow peaks. This phenomenology can be understood in terms of the interference of the emission from the different spatial positions: in agreement with experimental observations, the spatial profile of the condensate [Fig. 2(b)] consists, in fact, of several, yet mutually coherent spots connected by lower density regions.

The disorder is, however, not able to spoil the outward radial flow pattern which, despite some local distortions, remains clearly visible in the figure. The presence of a nontrivial phase profile is responsible for the noncentrosymmetric $\mathbf{k}$-space pattern and, in particular, for the $\mathbf{k}\neq 0$ position of the main peak. This is a clear signature of the nonequilibrium nature of the polariton condensate.

V. SMALL EXCITATION SPOT

The properties of the polariton condensate are completely different if a small excitation spot is used. Even though the local density approximation can no longer be performed, exact analytical predictions for the condensate wave function can still be obtained in the region far outside the pump spot. In this region, the condensate density is very small and polaritons no longer feel the repulsive potential, so that the radial part of the GPE (1) reduces to a linear Helmholtz equation of the form

$$\frac{\hbar}{2m}\nabla_{\mathbf{r}}^2\psi+\left(\omega_c-\omega_0+i\frac{\gamma_c}{2}\right)\psi=0, \tag{11}$$

whose converging solution for $r\to\infty$ has to be chosen. The frequency ω_c is fixed by the dynamics in the excitation region, and its analytical determination goes beyond the scope of the present work. The solution to the Helmholtz equation has the simple analytic expression $\psi(r)=H_0^{(1)}(\tilde{k}_c r)$, in terms of the first kind Hankel function $H_\nu^{(1)}$. The complex wave vector is

$$\tilde{k}_c=\sqrt{\frac{2m}{\hbar}\left(\omega_c-\omega_0+\frac{i\gamma_c}{2}\right)}. \tag{12}$$

From the asymptotic expansion of $H_\nu^{(1)}$, one immediately gets to the exponential decay

$$\psi(r\to\infty)\propto\frac{1}{\sqrt{r}}\exp(-\kappa_{pen}r) \tag{13}$$

with a spatial rate

$$\kappa_{pen}=\mathrm{Im}[\tilde{k}_c]\simeq\gamma_c/2v_c \tag{14}$$

and a propagation speed $v_c=\hbar k_c/m$, with

$$k_c = \mathrm{Re}[\tilde{k}_c] \simeq \sqrt{2m(\omega_c - \omega_0)/\hbar}. \quad (15)$$

Note that the limit $\gamma_c \to 0$ of the present theory does not correspond at all to the equilibrium state of trapped condensates. In a broad sense, it rather reminds us of the physics of the expansion of a trapped condensate once the trap potential has been switched off.[10]

These analytical considerations are accurately confirmed by a full numerical integration of Eqs. (1) and (2) for a small pump spot $\sigma_p = 1$ μm, whose results are summarized in the plots in the right column of Fig. 1. As the pump laser spot σ_p is much smaller than the characteristic propagation length κ_{pen}^{-1}, most of the polaritons are found outside the excitation region and are ballistically propagating in the outward direction.

The k-space emission then concentrates on the ring of radius k_c; the contribution from the central excitation region provides the weak pedestal at $k < k_c$, while almost no emission is present for $k > k_c$. The (k,E) pattern is analogously peaked around $(\pm k_{c0}, \hbar\omega_c)$ and shows a weaker pedestal on the horizontal segment at $E = \hbar\omega_c$ contained inside the free polariton dispersion. Qualitative agreement of these results with experimental observations in Fig. 1 of Ref. 1 is excellent: the ring structure is recovered as well as the relation between the emission frequency ω_c and the wave vector k_c.

VI. EFFECT OF NONCONDENSATE POLARITONS

All the calculations presented so far were based on a mean-field theory where the quantum polariton field was replaced by a $\mathbb{C}$ number and the contribution of the fluctuating noncondensed polaritons was mostly neglected apart from its contribution to the expelling potential. This approximation is a widespread one of the theory of Bose-Einstein condensates and has been proven to give accurate results in most cases of dilute gases that are reasonably far from the critical BEC temperature. To verify its validity for polariton condensates, we extended our calculations to the noncondensed polaritons by including a noise term in the motion equation (1).

Such a stochastic approach can be rigorously derived within the quasiprobability formalism of quantum optics and laser theory.[33] Recently, it was successfully applied to polariton systems to characterize the parametric luminescence from semiconductor microcavities[34] and, in particular, its fluctuations around the optical parametric threshold.[35] A complete report of the predictions of such a method for the correlation functions of the noncondensed fraction will appear in a forthcoming publication together with a full discussion of all the technicalities of the Wigner method related to the zero-point occupation and the different time commutators. Here, we will limit ourselves to those issues that directly concern the spatial and spectral shapes of polariton condensates.

Both damping and gain contribute to the noise terms in the stochastic equations of motion of Wigner representation. As numerical calculations are performed on a discrete grid of lattice points, the white noise term on the right hand side of the spatially discretized motion equation (1) has the following form:

$$d\psi_{stoch}(\mathbf{r}_i) = \sqrt{\frac{\gamma_c + R[n_R(\mathbf{r}_i)]}{4\Delta V}}\, dW_i, \quad (16)$$

where dW_i is a Gaussian random variable with white-noise correlation functions $\langle dW_i dW_j \rangle = 0$ and $\langle dW_i^* dW_j \rangle = 2\delta_{i,j} dt$. In order for the stochastical classical field theory to be accurate, the volume ΔV of the elementary cell of the numerical integration lattice has to be chosen such that $\gamma_c \gg g/\Delta V$. For the actual value of the polariton-polariton interaction constant, this condition can be satisfied without losing any relevant physics.[35]

Numerical results are shown in Fig. 3: the main conclusion that one can draw from it is that the spectral shape of the configurations considered in Fig. 1 remains qualitatively unaltered when noise is added. The only effect of fluctuations is to add a noncondensed population and to broaden the features of the (k,E) emission pattern, in agreement with the experimental observations of Refs. 1 and 32, in particular, Fig. 8.9.

In the case of the small excitation spot shown in Figs. 3(a) and 3(b), note how the emission pattern due to the noncondensed polaritons is not blueshifted with respect to the linear regime dispersion: this is easily explained by the fact that most of the incoherent polaritons are found outside of the high-density region. The physics is slightly more complicated in the case of a large excitation spot shown in Figs. 3(e) and 3(f): in the low-momentum region, the incoherent polaritons are distributed on a wide range of energies between the lower polariton branch and the condensate energy. On the other hand, they are mostly concentrated on the linear dispersion for high momenta. This behavior can be understood in terms of the blueshift now being a slowly varying function of the spatial positions. High-energy noncondensed polaritons travel for long distances and, therefore, spend most of their lifetime in the low-density external region. On the other hand, the low-energy ones are distributed among the various parts of the cloud and, therefore, experience a wide range of different values of the blueshift.

VII. CONCLUSIONS

In conclusion, we have developed a full theory of the spatial and spectral shape of polariton Bose-Einstein condensates that is able to explain the peculiar features observed in recent experiments:[1,2,32] signatures of the unique nonequilibrium nature of polariton condensates are identified in comparison to the standard case of condensates at equilibrium. Under the combined effect of pumping and losses, the stationary state of the condensate is, in fact, characterized by a steady flow in the outward radial direction as a consequence of the repulsive interactions and coherent polaritons can ballistically propagate outside the excitation spot.

All the qualitative features have been checked to be generic and robust with respect to changes in the model parameters and in the details of the pumping spot profile. Wigner–Monte Carlo numerical simulations indicate that the physical picture remains qualitatively unaltered when the noncondensate polaritons are included in the model.

The agreement of the results of our generalized Gross–Pitaevskii approach with experiments is promising for the

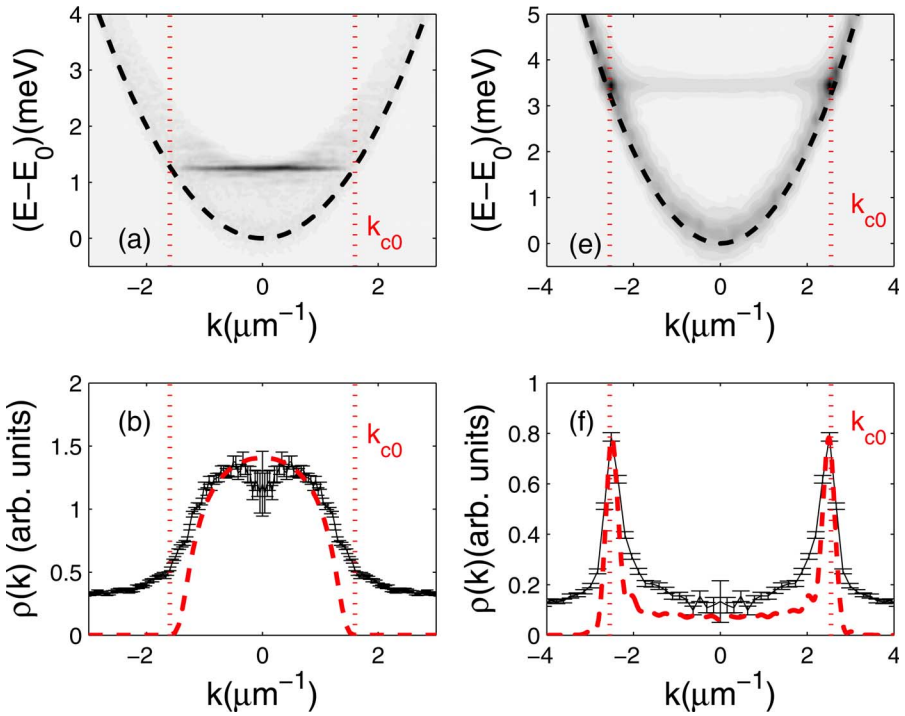

FIG. 3. (Color online) Wigner–Monte Carlo results (full line with error bars) for [(a) and (e)] the momentum space polariton distribution and [(b) and (f)] the (k,E) emission patterns including the noncondensed polaritons for [(a) and (b)] large and [(e) and (f)] small spot sizes, respectively. For comparison, the dashed line shows the mean-field momentum distribution. Same parameters as in the corresponding panels of Fig. 1.

application of the present model to more complex geometries that may be relevant in the design of polariton lasers based on suitably patterned structures. From the theoretical point of view, the next step will be an extensive campaign of Wigner–Monte Carlo simulations, including the fluctuations around the mean-field to fully characterize the condensate coherence properties and, eventually, the critical properties in the vicinity of the nonequilibrium phase transition.

Note added. Recently, a preprint[36] has appeared where similar issues are addressed from a slightly different perspective.

ACKNOWLEDGMENTS

Stimulating discussions with M. Richard, A. Baas, J. Keeling, D. Le Si Dang, D. Sarchi, V. Savona, M. Szymańska, P. Eastham, J. Tempere, and J. Devreese are gratefully acknowledged. This research has been supported financially by the FWO-V Projects No. G.0356.06 and No. G.0115.06, and the Special Research Fund of the University of Antwerp, BOF NOI UA 2004. M.W. acknowledges financial support from the FWO-Vlaanderen. I.C. acknowledges the hospitality at the Centre Emile Borel of the Institut Henri Poincaré and the financial support from CNRS.

[1] M. Richard, J. Kasprzak, R. Romestain, R. André, and L. S. Dang, Phys. Rev. Lett. **94**, 187401 (2005).
[2] M. Richard, J. Kasprzak, R. André, R. Romestain, L. S. Dang, G. Malpuech, and A. Kavokin, Phys. Rev. B **72**, 201301(R) (2005).
[3] J. Kasprzak, M. Richard, S. Kundermann, A. Baas, P. Jeambrun, J. M. J. Keeling, F. M. Marchetti, M. H. Szymanska, R. André, J. L. Staehli, V. Savona, P. B. Littlewood, B. Deveaud, and L. S. Dang, Nature (London) **443**, 409 (2006).
[4] H. Deng, D. Press, S. Götzinger, G. S. Solomon, R. Hey, K. H. Ploog, and Y. Yamamoto, Phys. Rev. Lett. **97**, 146402 (2006).
[5] R. Balili, V. Hartwell, D. Snoke, L. Pfeiffer, and K. West, Science **316**, 1007 (2007).
[6] S. Christopoulos, G. Baldassarri Höger von Högersthal, A. Grundy, P. G. Lagoudakis, A. V. Kavokin, J. J. Baumberg, G. Christmann, R. Butté, E. Feltin, J. F. Carlin, and N. Grandjean, Phys. Rev. Lett. **98**, 126405 (2007).
[7] For a review, see J. Keeling, F. M. Marchetti, M. H. Szymanska, and P. B. Littlewood, Semicond. Sci. Technol. **22**, R1 (2007).
[8] BEC effects in a solid-state context have been observed also in dilute gases of magnons [see, e.g., T. Nikuni, M. Oshikawa, A. Oosawa, and H. Tanaka, Phys. Rev. Lett. **84**, 5868 (2000); S. O. Demokritov, V. E. Demidov, O. Dzyapko, G. A. Melkov, A. A. Serga, B. Hillebrands, and A. N. Slavin, Nature (London) **443**, 430 (2006)]; and of exciton in bilayer electron gases [J. P. Eisenstein and A. H. MacDonald, Nature (London) **432**, 691 (2004)].
[9] A. Imamoglu, R. J. Ram, S. Pau, and Y. Yamamoto, Phys. Rev. A **53**, 4250 (1996); D. Snoke, Nature (London) **443**, 403 (2006).
[10] L. P. Pitaevskii and S. Stringari, *Bose-Einstein Condensation* (Clarendon, Oxford, 2003).
[11] W. Lamb, Phys. Rev. **134**, A1429 (1964).
[12] I. Carusotto and C. Ciuti, Phys. Rev. Lett. **93**, 166401 (2004); C. Ciuti and I. Carusotto, Phys. Status Solidi B **242**, 2224 (2005); I. Carusotto and C. Ciuti, Phys. Rev. B **72**, 125335 (2005).
[13] M. Wouters and I. Carusotto, Phys. Rev. B **74**, 245316 (2006); M. H. Szymańska, J. Keeling, and P. B. Littlewood, Phys. Rev. Lett. **96**, 230602 (2006); M. Wouters and I. Carusotto, Phys.

Rev. A **76**, 043807 (2007).
[14] M. Wouters and I. Carusotto, Phys. Rev. Lett. **99**, 140402 (2007).
[15] A. J. Leggett, Rev. Mod. Phys. **73**, 307 (2001).
[16] First attempts [T. D. Doan, H. T. Cao, D. B. Tran Thoai, and H. Haug, Phys. Rev. B **74**, 115316 (2006)] based on the Boltzmann equation with a momentum dependent polariton lifetime do not seem to be able to account for the dramatic dependence on the pump spot size.
[17] D. Porras, C. Ciuti, J. J. Baumberg, and C. Tejedor, Phys. Rev. B **66**, 085304 (2002).
[18] F. Tassone and Y. Yamamoto, Phys. Rev. B **59**, 10830 (1999).
[19] T. D. Doan, H. T. Cao, D. B. Tran Thoai, and H. Haug, Phys. Rev. B **72**, 085301 (2005).
[20] G. Malpuech, A. Kavokin, A. Di Carlo, and J. J. Baumberg, Phys. Rev. B **65**, 153310 (2002).
[21] D. Sarchi and V. Savona, Phys. Rev. B **75**, 115326 (2007).
[22] P. Schwendimann and A. Quattropani, Phys. Rev. B **74**, 045324 (2006).
[23] Y. G. Rubo, F. P. Laussy, G. Malpuech, A. Kavokin, and P. Bigenwald, Phys. Rev. Lett. **91**, 156403 (2003); F. P. Laussy, G. Malpuech, A. Kavokin, and P. Bigenwald, *ibid.* **93**, 016402 (2004).
[24] M. C. Cross and P. C. Hohenberg, Rev. Mod. Phys. **65**, 851 (1993).
[25] J. M. Chomaz, Annu. Rev. Fluid Mech. **37**, 357 (2005).
[26] R. Kuszelewicz, I. Ganne, I. Sagnes, G. Slekys, and M. Brambilla, Phys. Rev. Lett. **84**, 6006 (2000).
[27] C. Ciuti, P. Schwendimann, and A. Quattropani, Semicond. Sci. Technol. **18**, S279 (2003).
[28] P. Lugan, D. Sarchi, and V. Savona, Phys. Status Solidi C **3**, 2428 (2006).
[29] Although the present knowledge of these parameters is quite poor, we have checked that the conclusions of our analysis do not depend on the specific values actually used in the simulations. The only quantity that matters is the total blueshift $\omega_c - \omega_0$ of the condensate frequency, a quantity which is easily extracted from experimental data.
[30] Although the loss rate of bottleneck polaritons is generally of the same order of magnitude as the condensate one, the effective relaxation rate γ_R is much faster thanks to the thermalization of bottleneck polaritons with the much larger bath of high-energy excitations created by the pump laser. A detailed discussion on these issues is postponed to a forthcoming publication.
[31] Note that this is not always the case if, e.g., a trapped system ($V_{ext} = m\omega_{tr}^2 r^2/2$) with a spatially uniform pump $P(\mathbf{r}) = P_0$ is considered: the instability of some surface modes may prevent, in fact, the system from getting to the stationary solution at a single ω_c considered here (Ref. 36).
[32] M. Richard, Ph.D. thesis, Université Joseph Fourier, 2004 (http://tel.archives-ouvertes.fr/tel-00009088).
[33] P. Zoller and C. W. Gardiner, *Quantum Noise* (Springer, New York, 2000).
[34] A. Verger, I. Carusotto, and C. Ciuti, Phys. Rev. B **76**, 115324 (2007).
[35] I. Carusotto and C. Ciuti, Phys. Rev. B **72**, 125335 (2005).
[36] J. Keeling and N. G. Berloff, arXiv:0706.3686 (unpublished).